

Fabrication of Schottky barrier diodes utilizing carboxylate bridged trinuclear mixed valence cobalt(III/II/III) complexes of tetradentate N₂O₂ donor reduced Schiff base ligands

Sudip Bhunia,^a Pubali Das,^b Snehasis Banerjee,^c Rosa M. Gomila,^d Michael G. B. Drew,^e Antonio Frontera,^d Partha Pratim Ray^b and Shouvik Chattopadhyay^{a,*}

^a*Department of Chemistry, Inorganic Section, Jadavpur University, Kolkata 700032, India. E-mail: shouvik.chattopadhyay@jadavpuruniversity.in; shouvik.chem@gmail.com; Tel: +91 3324572941*

^b*Department of Physics, Jadavpur University, Kolkata 700032, India. E-mail: partha@phys.jdvu.ac.in; Fax: +91 3324138917*

^c*Department of Higher Education, (University Branch) Government of West Bengal, Bikash Bhavan, Salt Lake, Kolkata-91, India.*

^d*Departament de Química, Universitat de les Illes Balears, Crta de valldemossa km 7.7, 07122 Palma de Mallorca (Balears), SPAIN. E-mail: toni.frontera@uib.es*

^e*School of Chemistry, The University of Reading, P.O. Box 224, Whiteknights, Reading RG6 6AD, United Kingdom*

Synthesis of Schiff bases, H_2L^a {2,2'-[(2,2-dimethyl-1,3-propanediyl)bis(nitrilomethylidyne)]bis[phenol]} and H_2L^b {2,2'-[(2,2-dimethyl-1,3-propanediyl)bis(nitriloethylidyne)]bis[phenol]}

The N_2O_2 donor Schiff base ligands, H_2L^a and H_2L^b , were prepared by refluxing 2,2-dimethylpropane-1,3-diamine (0.2 mL, ~2 mmol) respectively with salicylaldehyde (0.4 mL, ~4 mmol) and 2-hydroxyacetophenone (0.4 mL, ~4 mmol) in methanol (10 mL) for ca. 1 h. Both the ligands were not isolated, but were reduced with borohydride to get the corresponding reduced analogues of these Schiff bases (vide infra).

Synthesis of the reduced Schiff base ligands, H_2L^1 {1,3-Bis(2-hydroxybenzylamino)2,2-dimethylpropane} and H_2L^2 {2,2'-[1,1'-(Propane-2,2-diyl-diimino)diethylidene]diphenol}

The methanol solution of the Schiff base, H_2L^a , was cooled to 0°C, followed by the addition of excess solid sodium borohydride with constant stirring. The resulting solution was acidified with glacial acetic acid and placed under reduced pressure in a rotary evaporator at ~65°C. The residue was dissolved in water (5 mL) and extracted with dichloromethane (5 mL) using a separating funnel. A little amount of sodium bi-carbonate was added to neutralize the extra acidic concentration. Finally, the ligand solution in dichloromethane was dried using anhydrous sodium acetate and the reduced Schiff base ligand, H_2L^1 was collected in methanol. H_2L^2 was prepared in a similar method starting from the Schiff base, H_2L^b .

Physical measurement

Elemental analyses (carbon, hydrogen and nitrogen) were performed using a Perkin-Elmer 240C elemental analyzer. IR spectra in KBr (4500-500 cm^{-1}) were recorded with a Perkin-Elmer RX-1 FTIR spectrophotometer. Electronic spectra in acetonitrile were recorded on UV-Vis-spectrofluorometer, SHIMADZU (UV-1900i). Cyclic voltammetry was carried out using a MetrohmAutolab electrochemical analyzer in a potential range from -2.0 V to +2.0 V with a scan rate of 200 mVs^{-1} using glassy carbon as working electrode, Ag/AgCl as reference electrode and platinum wire as auxiliary electrode at ambient temperature (300 K) under argon (Ar) atmosphere. Thermo-gravimetric analyses (TGA) was carried out on a Perkin-Elmer pyris Diamond TG/DTA thermal analyzer under nitrogen atmosphere (flow rate: 50 $\text{cm}^3 \text{min}^{-1}$) with a heating rate of 10 $^\circ\text{C min}^{-1}$. The magnetic susceptibility measurements were done with an EG&PAR vibrating sample magnetometer, model 155 at room temperature and diamagnetic corrections were made using Pascal's constants. Effective magnetic moments were calculated using the formula $\mu_{\text{eff}} = 2.828(\chi_M T)^{1/2}$, where χ_M is the corrected molar susceptibility.

X-Ray crystallography

Suitable single crystals of the complexes were picked out and were mounted on a glass fibre. A 'Bruker D8 QUEST area detector' diffractometer equipped with graphite-monochromated Mo- K_α radiation ($\lambda = 0.71073 \text{ \AA}$). The molecular structures were solved by direct method and refined by full-matrix least squares on F^2 using the SHELX-16/6 package.^{S1} Non-hydrogen atoms were refined with anisotropic thermal parameters. The hydrogen atoms attached to oxygen atoms were located by difference Fourier maps and were kept at fixed positions. All other hydrogen atoms were placed in their geometrically idealized positions and constrained to ride on their parent atoms. Multi-scan absorption corrections were applied to the data using the program SADABS.^{S2}

Fabrication and characterization of ITO/Complex/Al based Schottky Barrier Diode

Thin film semiconducting devices were constructed using prepared materials and utilized to characterize materials electrically. For this research, three glass substrates coated with ITO (Indium Tin Oxide) were employed. They were initially cleaned repeatedly in 2-propanol, acetone, and distilled water. Glass substrates were air dried naturally in a N₂ atmosphere. Using DMF as the dispersive medium, three different homogeneous dispersions of prepared molecules were produced through ultra-sonication. The dispersions were applied to the conducting side of three different ITO coated glasses using a spin coating equipment at a speed of 1000 rpm for three minutes each. After the films had finished vacuum drying, their thickness was tested with a surface profiler, and it was found to be almost one micrometer. Aluminum (Al) metal was added to the thin films using a vacuum coating unit (HINDHIVAC) and an electron beam gun evaporation method. Finally, Metal Semiconductor (MS) junction were built with a sandwich pattern of ITO/complex **1**/Al, ITO/complex **2**/Al, and ITO/complex **3**/Al, with Al acting as the metal electrode. The effective diode area (A) was kept as $7.065 \times 10^{-6} \text{ m}^2$ with a shadow mask during metal deposition.

For electrical characterization, the current-voltage (I-V) characteristics of the devices were measured in dark environments using a Keithley 2635B source meter. All preparations and measurements were performed at room temperature and under normal circumstances.

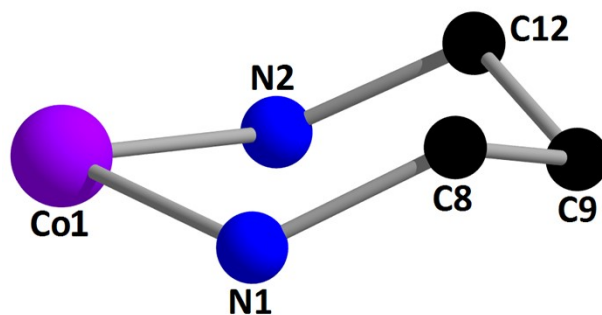


Figure S1: Chair conformation of a saturated six-membered chelate ring in the complex 2. Only selected atoms have been shown.

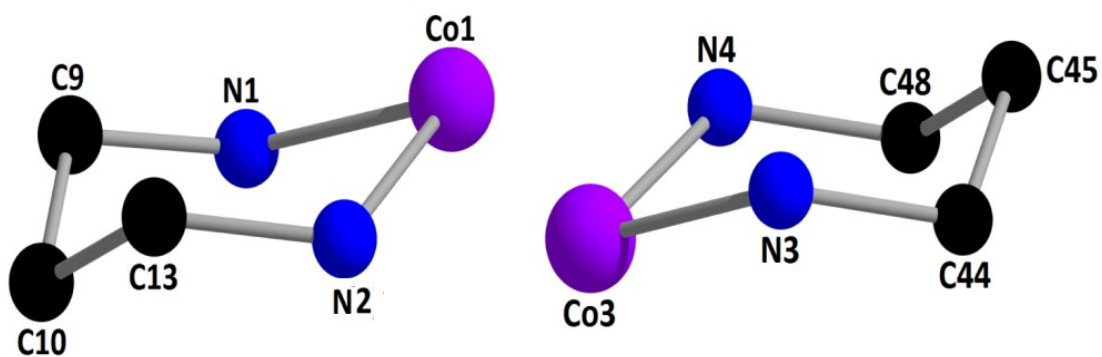


Figure S2: Chair conformation of the saturated six-membered chelate rings in complex 3. Only selected atoms have been shown.

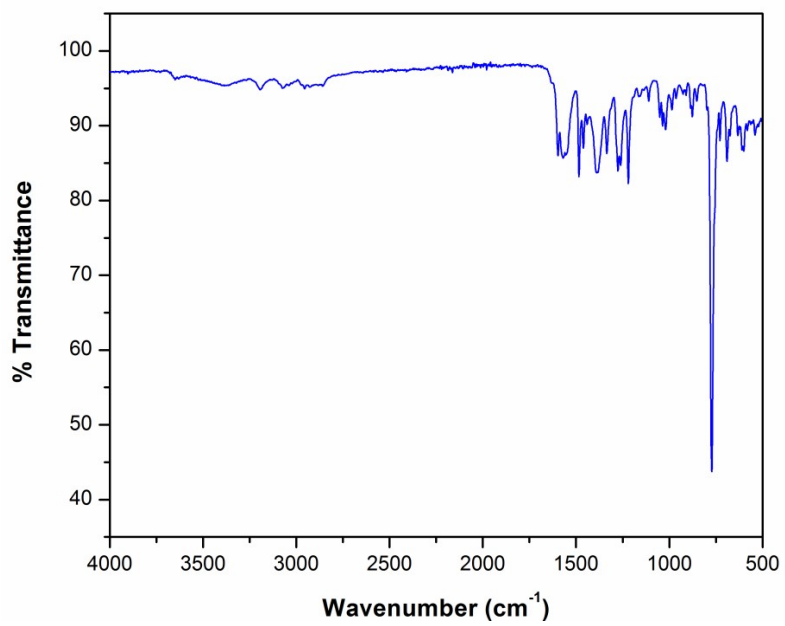


Figure S3: IR spectrum of complex 1.

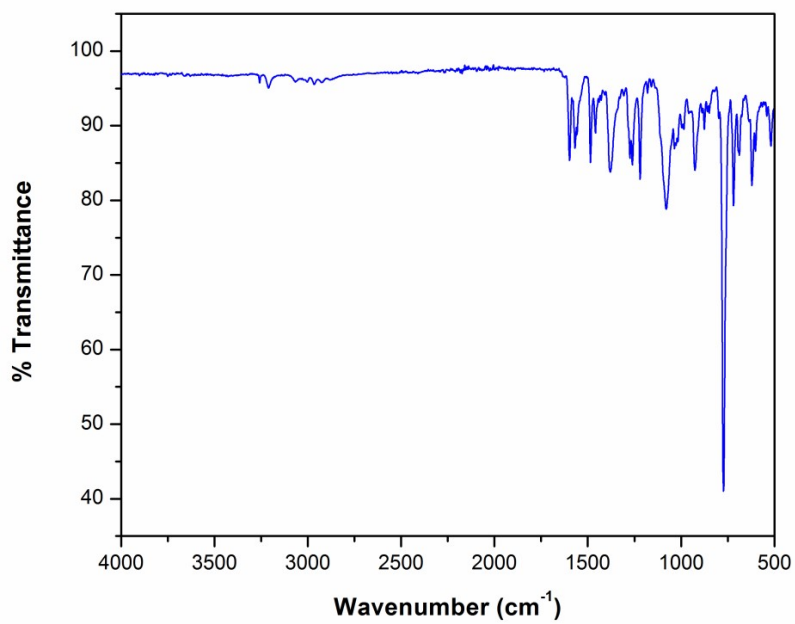


Figure S4: IR spectrum of complex 2.

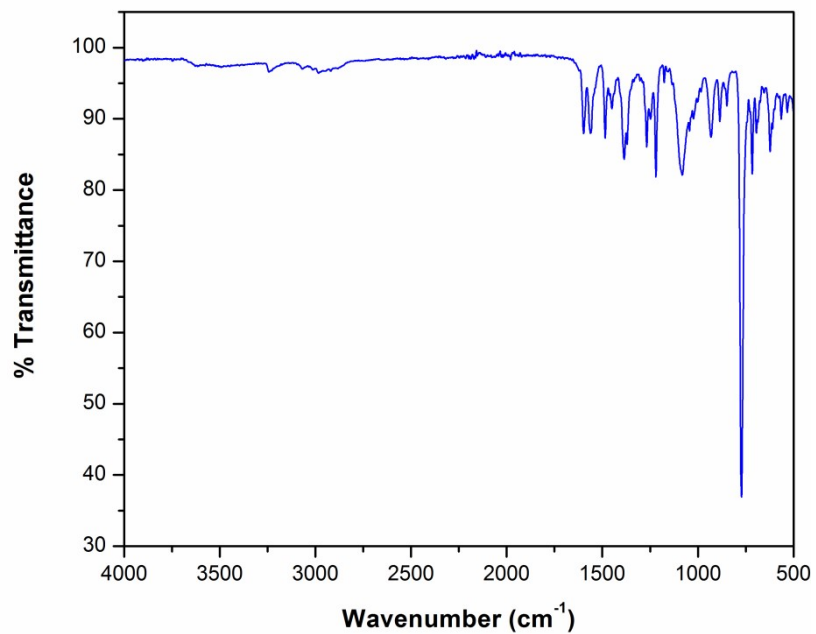


Figure S5: IR spectrum of complex **3**.

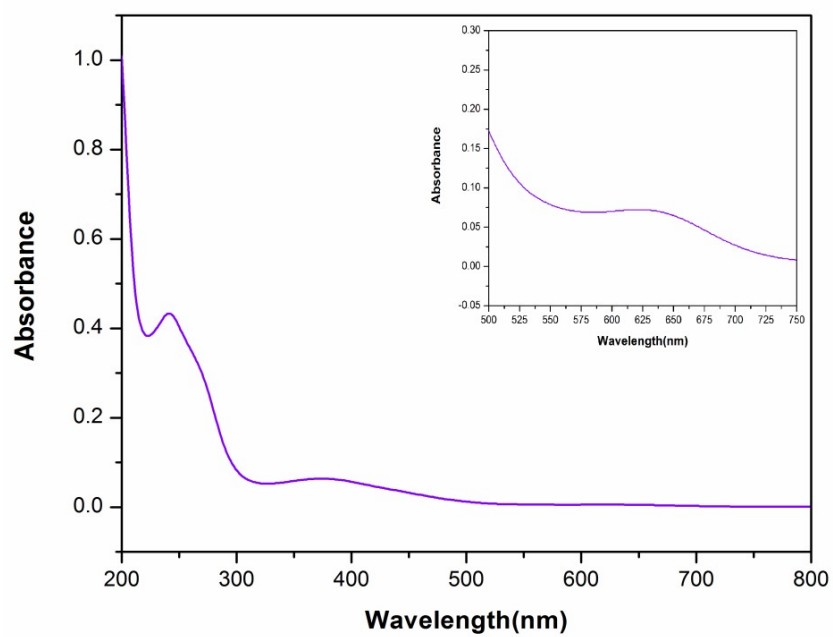


Figure S6: Electronic spectrum of complex **1** in acetonitrile. Inset shows the absorption band for low spin cobalt(III) center in the complex.

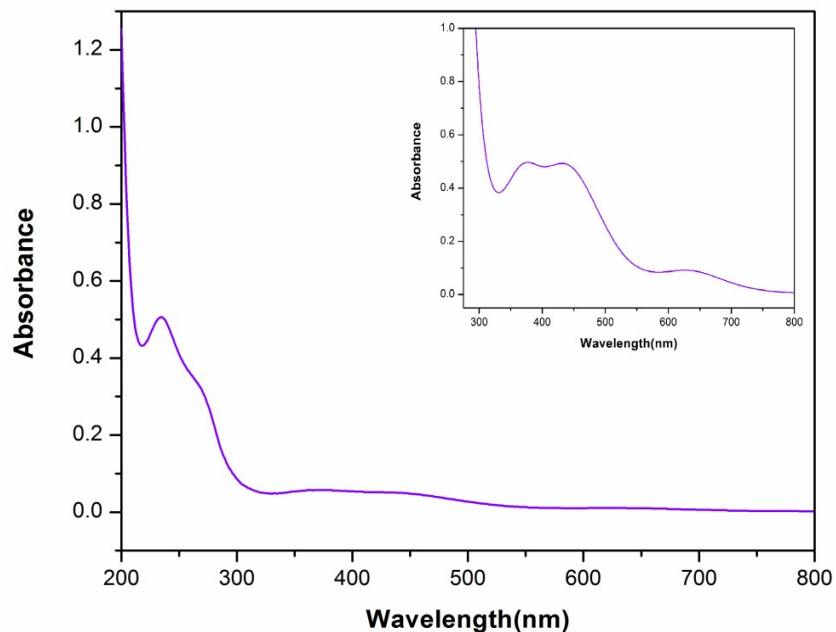


Figure S7: Electronic spectrum of complex **2** in acetonitrile. Inset shows the absorption bands for LMCT and low spin cobalt(III) center in the complex.

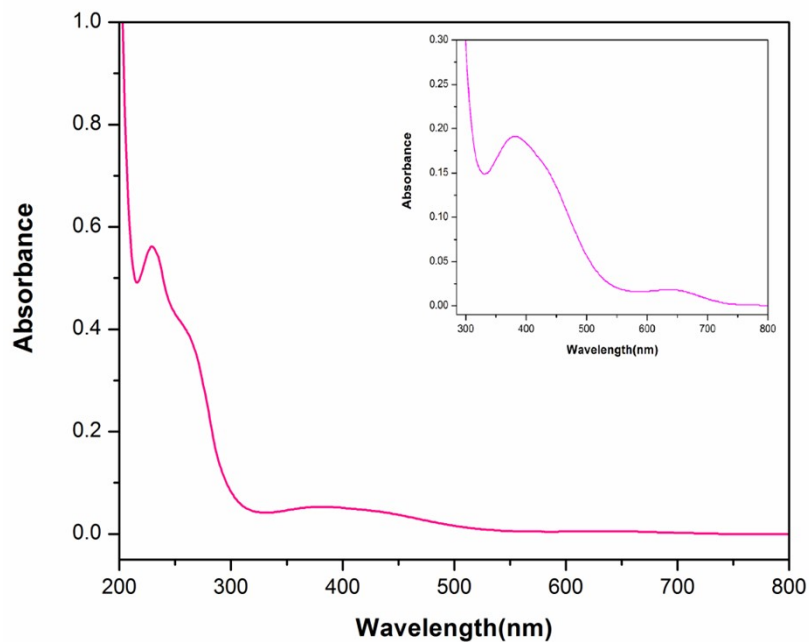


Figure S8: Electronic spectrum of complex **3** in acetonitrile. Inset shows the absorption bands for LMCT and low spin cobalt(III) center in the complex.

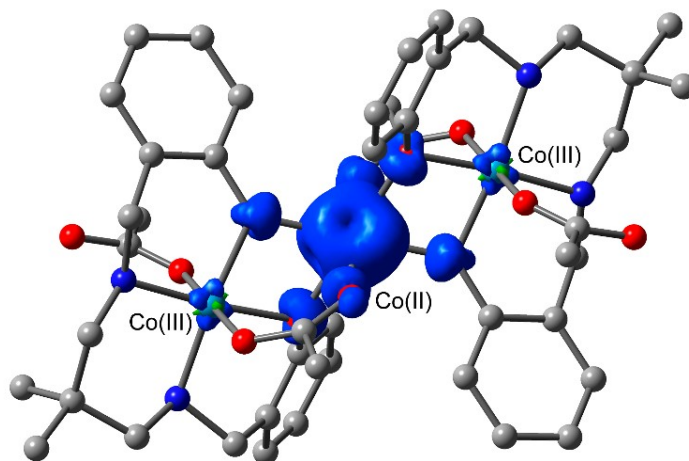


Figure S9: Spin density plot for complex **1** (isovalue 0.04 a.u.) at the RI-BP86-D3/def2-SVP level of theory.

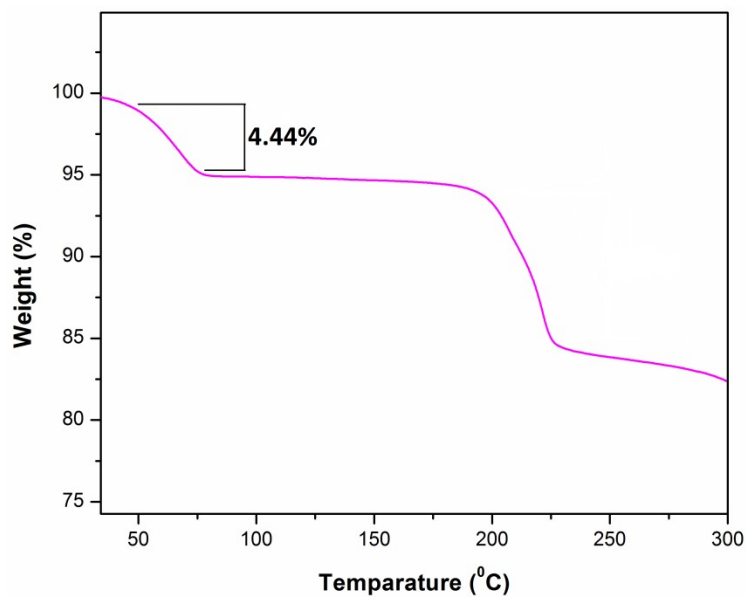


Figure S10: TGA plot (corresponding to the loss of two water molecules) of complex **1**.

Electrochemical studies

The redox behavior of the two synthesized complexes were analyzed by using cyclic voltammetry (CV) in DMF with 10^{-3} M of each complex containing tetrabutylammonium bromide (TBAB) as supporting electrolyte.

Cyclic voltammetric studies of all the complexes **1**, **2** and **3** display two one electron cyclic voltammetric responses. From them, one is quasi-reversible redox signal and another is irreversible redox signal. The quasi-reversible redox signal consists of an oxidation peak, E_{pa} (+1.49 V, +1.45 V and +1.42 V for complexes **1**, **2** and **3**, respectively) and a reduction peak, E_{pc} (+1.16 V, +1.17 V and +1.15 V for complexes **1**, **2** and **3**, respectively), whereas the irreversible signal consists only a reduction peak, E_{pc} (-0.96 V, -0.88 V and -0.82 V for complexes **1**, **2** and **3**, respectively). This quasi-reversible redox signal could be attributed to the $\text{Co}^{\text{II}} \rightarrow \text{Co}^{\text{III}}$ oxidation and the $\text{Co}^{\text{III}} \rightarrow \text{Co}^{\text{II}}$ reduction, whereas the irreversible signal could be attributed to the $\text{Co}^{\text{III}} \rightarrow \text{Co}^{\text{II}}$ reduction only.^{S3,S4} The cyclic voltammograms of all the complexes **1**, **2** and **3** are shown, respectively in Figures S11-S13. The similar patterns of cyclic voltammograms of all three complexes indicate the similarity of their structures. The results of cyclic voltammetry are similar to that of other trinuclear mixed valence complexes of cobalt, reported in literature. This serves as further evidences for similar structural and electronic properties. The detailed electrochemical data for all the complexes are given in Table S2.

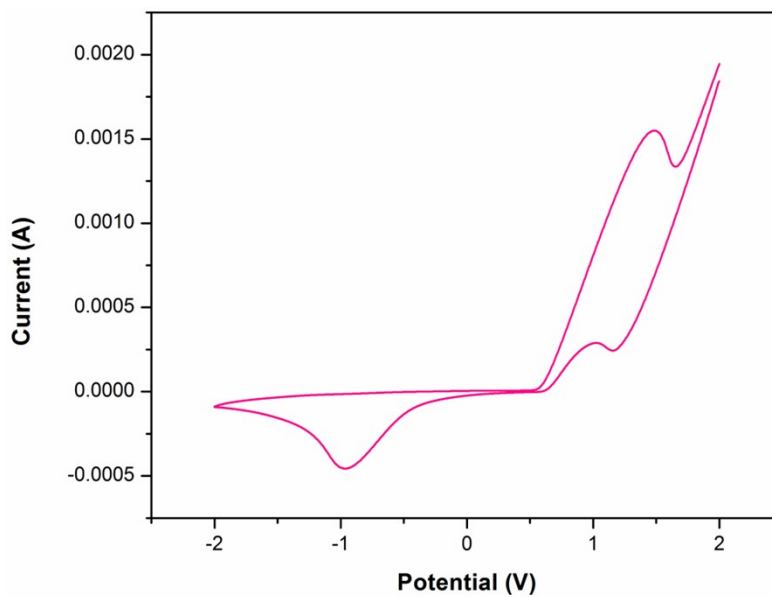


Figure S11: Cyclic voltammograms of the complex **1** in DMF (using. Ag/AgCl reference electrode).

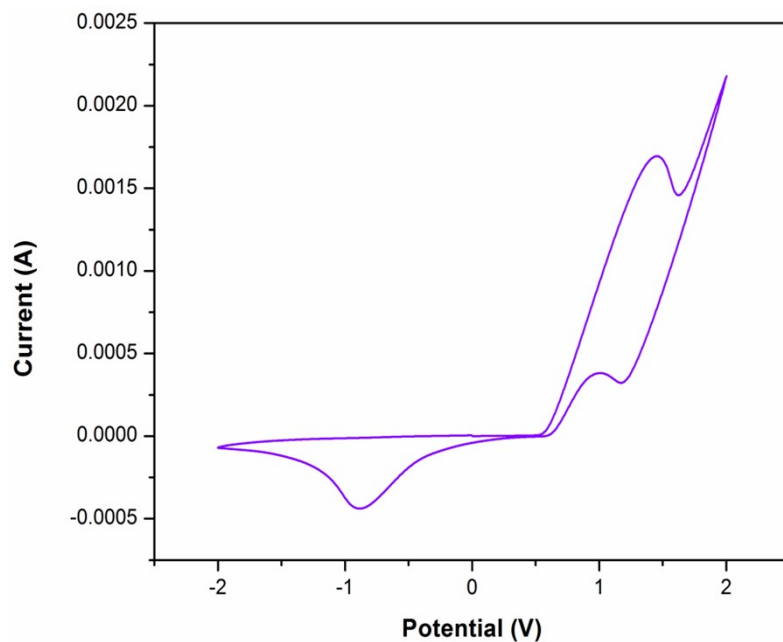


Figure S12: Cyclic voltammograms of the complex **2** in DMF (using. Ag/AgCl reference electrode).

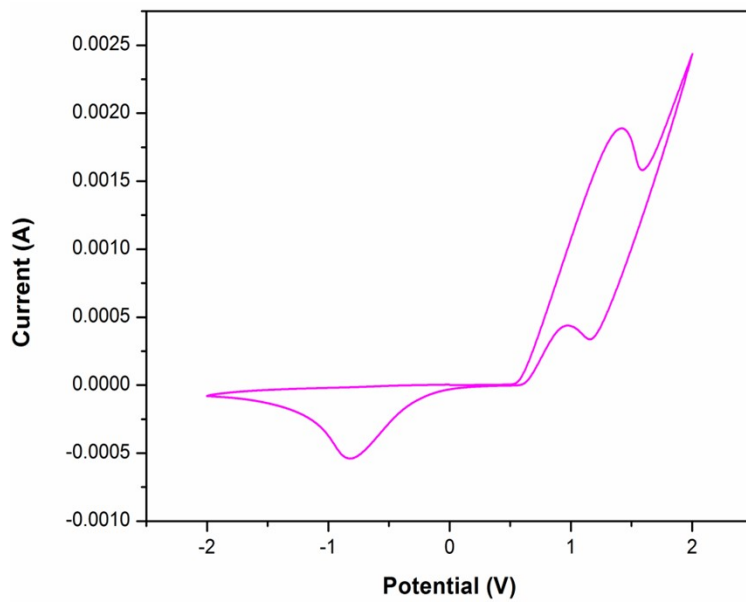


Figure S13: Cyclic voltammograms of the complex **3** in DMF (using. Ag/AgCl reference electrode).

Table S1: List of hydrogen bonds in complexes 1–3.

Complex	Atoms involved (D–H...A)	Distance D–H (Å)	Distance H...A (Å)	Distance D...A (Å)	Angle D–H...A (°)	Symmetry Operation
1	N(1)-H(1)···O(6A)	0.85(7)	1.95(7)	2.792(4)	170(7)	–
	N(1)-H(1)···O(5)	0.85(7)	2.40(7)	2.824(11)	112(6)	–
	N(1)-H(1)···O(5A)	0.85(7)	2.41(10)	2.83(6)	111(6)	–
	N(2)-H(2)···O(1W)	0.98	2.20	3.109(7)	154.6	–
	N(2)-H(2)···O(6B)	0.98	1.92	2.802(15)	147.9	–
	O(1W)-H(1WB)···O(3W)	0.85	1.84	2.573(14)	144.2	–
	O(2W)-H(2WA)···O(3W)	0.78	2.31	2.699(16)	112.1	3-X, 2-Y, -Z
	O(2W)-H(2WB)···O(6A)	0.86	2.16	2.787(8)	129.4	–
	O(3W)-H(3WA)···O(3W)	0.85	1.85	2.699(16)	178.8	3-X, 2-Y, -Z
2	N(1)-H(1N)···O(91)	0.96(8)	1.84(8)	2.70(2)	148(7)	–
	N(1)-H(1N)···O(91)	0.96(8)	2.23(8)	3.144(7)	158(7)	–
	C(12)-H(12A)···O(12)	0.97	2.57	3.487(10)	158.72	1-X, 1-Y, -Z
	C(13)-H(13B)···O(13)	0.97	2.61	3.434(13)	143.02	1-X, 1-Y, -Z
3	N(1)-H(1)···O(1A)	0.98	2.54	3.395(13)	145.2	1+X, Y, Z
	N(2)-H(2)···O(72)	0.98	2.04	2.92(2)	148.7	–
	N(2)-H(2)···O(11)	0.98	2.38	3.031(11)	123.1	–
	N(3)-H(3)···O(10)	0.98	2.63	3.503(16)	148.3	X, 3/2-Y, Z-1/2

	N(4)-H(4)···O(82)	0.98	1.98	2.874(15)	149.7	–
	N(4)-H(4)···O(13)	0.98	2.30	3.123(11)	141.5	X, 3/2-Y, Z-1/2

Table S2: Cyclic voltammetry data (V) for complexes **1–3** in DMF medium

Complex	Scan rate (mV s⁻¹)	E_{pa} (V) (Co^{II}→Co^{III})	E_{pc} (V) (Co^{III}→Co^{II})	E_{1/2} (V) (Co^{II}↔Co^{III})	ΔE_p (Co^{II}↔Co^{III})	E_{pc} (V) (Co^{III}→Co^{II})
1	200	+1.49	+1.16	+1.33	+0.33	-0.96
2	200	+1.45	+1.17	+1.31	+0.28	-0.88
3	200	+1.42	+1.15	+1.29	+0.27	-0.82

E_{1/2} denotes the half-wave potential. **E_{1/2} = (E_{pa} + E_{pc})/2** and **ΔE_p = (E_{pa} - E_{pc})**

References

S1 G. M. Sheldrick, *SHELXT. ActaCryst*, 2015, **71A**, 3–8.

S2 G.M. Sheldrick, SADABS, V2014/5, Software for Empirical Absorption Correction, University of Gottingen, Institute fur AnorganischeChemiederUniversitat, Gottingen, Germany, 1999–2003.

S3 S. Bhunia and S. Chattopadhyay, *Results in Chemistry*, 2023, **5**, 100701.

S4 M. Das and S. Chattopadhyay, *Polyhedron*, 2013, **50**, 443–451.